

Thermal gas rectification using a sawtooth channel

S Solórzano,¹ N.A.M. Araújo,^{2,*} and H.J. Herrmann^{1,3}

¹*Computational Physics for Engineering Materials, Institut f. Baustoffe (IfB), ETH Zurich, Wolfgang-Pauli-Street 27, 8093 Zurich, Switzerland*

²*Departamento de Física, Faculdade de Ciências, Universidade de Lisboa, P-1749-016 Lisboa, Portugal, and Centro de Física Teórica e Computacional, Universidade de Lisboa, P-1749-016 Lisboa, Portugal*

³*Departamento de Física, Universidade Federal do Ceará, 60451-970 Fortaleza, Ceará, Brazil*

We study the rectification of a two-dimensional thermal gas in a channel of asymmetric dissipative walls. For an ensemble of smooth Lennard-Jones particles, our numerical simulations reveal a non-monotonic dependence of the flux on the thermostat temperature, channel asymmetry, and particle density, with three distinct regimes. Theoretical arguments are developed to shed light on the functional dependence of the flux on the model parameters.

I. INTRODUCTION

Systems where fluctuations are rectified into directed motion are known as Brownian motors or ratchet devices [1, 2]. According to the second law of thermodynamics, these systems ought to be impossible in equilibrium [2, 3]. This is why broken spatial symmetry and non equilibrium conditions are a key feature for their operation [4, 5]. Brownian motors are relevant in a number of situations from biological processes to devices for particle segregation [6–9] and transport [10–12]. For instance, asymmetric objects (e.g., wedge shapes) immersed in a granular gas tend to move [13, 14] or rotate [15–18] in a preferential direction, provided that particle/object collisions are dissipative. Also, granular particles enclosed in a vibrating sawtooth-shaped channel flow along a preferential direction defined by the asymmetry of the channel [19]. Similar results are also observed for microscopic particles in an asymmetric channel under the action of a pulsating potential [7]. There are also various examples of active matter systems ranging from bacteria at microscopic scale [20–22], to centimeter scale bots [23], up to pedestrians [24] where rectification can be induced by spatial asymmetries. Although these systems rectify the motion of the particles, they still require either a pulsating potential or active particles.

In the present work, we show that the motion of a gas of Lennard-Jones particles can be rectified without external pulsating potentials only by means of dissipation and broken spatial asymmetry. To this end, we consider a two-dimensional gas of particles in a fixed (not moving) asymmetric sawtooth-shaped channel and study how the overall flux depends on the different model parameters. We expect that this idea can find applications in fields such as microfluidic or lab on a chip set ups.

The paper is organized as follows. In Section II, the model and methods are introduced. The results are discussed in Section III and we draw some conclusions in Section IV.

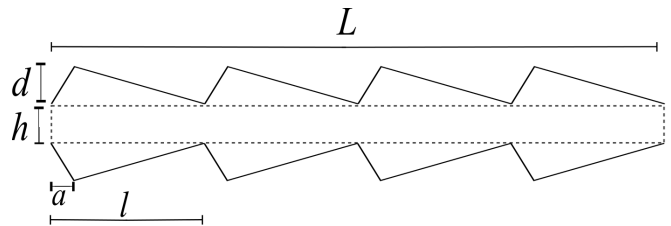


FIG. 1. Schematic representation of the channel of size L , with $N = 4$ cells. The shape of each cell is characterized by four lengths: the linear length l , the aperture size h , and the horizontal position a and height d of the peak. The dashed lines delimit the region where particles are initially released.

II. MODEL AND METHODS

We consider a two-dimensional sawtooth channel of linear length L consisting of a sequence of N equal cells, as represented in Fig. 1, with periodic boundary conditions along the horizontal axis. The geometry of the channel is characterized by four lengths: the length of each cell $l = L/N$, the aperture size h , and the horizontal position a and height d of the edge. To systematically study the dependence on the asymmetry of the channel, we fix h and define the adimensional asymmetry coefficient α as,

$$\alpha = 1 - 2 \frac{a}{l}, \quad (1)$$

where $\alpha \in [-1, 1]$. For $\alpha = 0$ the channel is symmetric with respect to the vertical axis, while for $\alpha = \pm 1$ the cells look triangular. We classify channels of negative and positive α as left and right asymmetric, respectively.

We consider a gas of particles interacting pairwise, where the force of particle j on particle i is conservative and given by $\mathbf{F}_{ij} = -\nabla_i U_{\text{LJ}}$. U_{LJ} is the 12 – 6-Lennard-Jones potential,

$$U_{\text{LJ}}(r_{ij}) = 4\epsilon \left[\left(\frac{\sigma}{r_{ij}} \right)^{12} - \left(\frac{\sigma}{r_{ij}} \right)^6 \right], \quad (2)$$

parameterized by ϵ and σ , where $r_{ij} = |\mathbf{r}_j - \mathbf{r}_i|$, and \mathbf{r}_i and \mathbf{r}_j are the positions of particles i and j , respectively.

* nmaraujo@fc.ul.pt

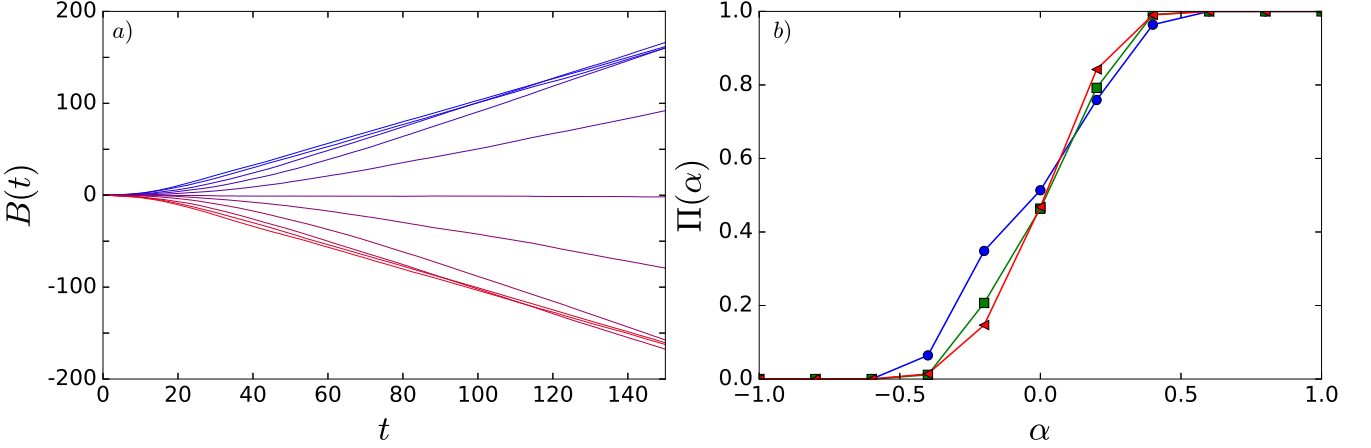


FIG. 2. (Color online) a) Time evolution of the balance $B(t)$ for different values of $\alpha = \{-1.0, -0.8, -0.6, -0.4, -0.2, 0, 0.2, 0.4, 0.6, 0.8, 1.0\}$ (from bottom to top). Results are averages over 500 samples of systems of 100 particles at a thermostat temperature $T = 2.5$ and $\gamma = 1$. b) Fraction of samples Π for which $B(t) > 0$, for $T = 2.5$, $\rho = 0.143$, and $N = 250$ (blue circles), $N = 500$ (green squares), $N = 1000$ (red triangles).

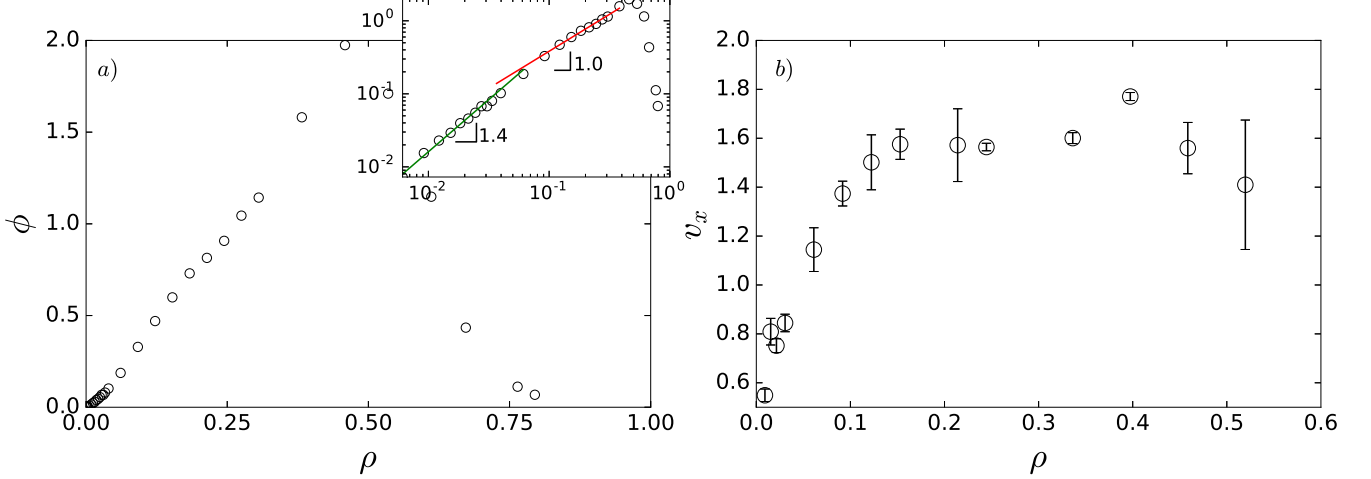


FIG. 3. (Color online) a) Flux ϕ as a function of the density ρ , for $T = 2.5$ and $\alpha = 1$. The two initial regimes are shown in the inset in a double logarithmic plot, where the dashed lines represent the power-law fits, $\phi \sim \rho^\beta$, with $\beta = 1.47 \pm 0.07$ and $\beta = 1.01 \pm 0.04$ for the low and intermediate density regimes, respectively. b) Average horizontal component of the particle velocity (v_x) as a function of the density, for the same set of parameters.

The force \mathbf{F}_{iw} of the wall on a particle i is described as the superposition of two contributions: a conservative force, \mathbf{F}_{iw}^c , and a dissipative one, \mathbf{F}_{iw}^d . The conservative force is described as a Lennard-Jones interaction with the closest point on the wall, with the same ϵ and σ of the particle/particle interaction. The dissipative force is given by,

$$\mathbf{F}_{\text{iw}}^d = -\gamma (\dot{\mathbf{r}}_i \cdot \hat{\mathbf{n}}_{\text{iw}}) \hat{\mathbf{n}}_{\text{iw}} , \quad (3)$$

where $\hat{\mathbf{n}}_{\text{iw}} = \frac{\mathbf{r}_i - \mathbf{r}_w}{r_{iw}}$ is the unit vector pointing from the closest point on the wall \mathbf{r}_w to the particle i and $\gamma \geq 0$ is a friction constant. The particle/wall interaction is conservative for $\gamma = 0$ and dissipative otherwise. Interactions with the wall are truncated at a cutoff distance

$$d_c = 2.5\sigma .$$

We performed canonical molecular dynamics simulations, using the Nosé-Hoover thermostat [25–27]. Accordingly, the equation of motion of particle i is,

$$\ddot{\mathbf{r}}_i = \frac{1}{m_i} \left(\sum_{j \neq i} \mathbf{F}_{ij}(\mathbf{r}_{ij}) + \mathbf{F}_{\text{iw}} \right) + \mathbf{F}_{\text{NH}} , \quad (4)$$

where m_i is the particle mass and \mathbf{F}_{NH} is the force per unit of mass, resulting from the coupling with the thermostat [27], and $\mathbf{r}_{ij} = \mathbf{r}_j - \mathbf{r}_i$. For simplicity, we set $m_i \equiv m$ and consider reduced units, such that: mass is in units of m , distance in units of σ , and energy in units of ϵ . The equations of motion are integrated using

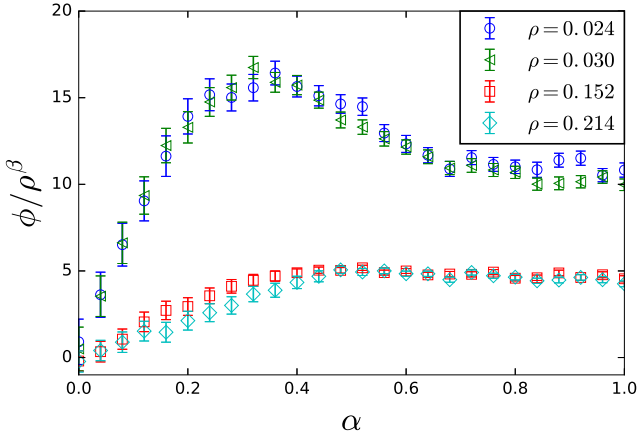


FIG. 4. (Color online) a) Flux ϕ rescaled by ρ^β as a function of α for $T = 2.5$ and different values of the density: $\rho = \{0.024, 0.030, 0.152, 0.214\}$, respectively, circles, triangles, squares, and diamonds. We rescaled the first two using $\beta = 1.47$ and the others using $\beta = 1.01$.

a fifth-order predictor corrector algorithm, with a time step $dt = 10^{-5}$ and we run the simulation up to $t = 165$.

To generate the initial configurations, all particles were released within the region delimited by the dashed lines in Fig. 1, with an initial velocity drawn from a uniform distribution of zero mean. Particles are thermalized at the thermostat temperature within the dashed region, considering periodic boundary conditions along the horizontal direction and reflective top and bottom boundaries, without interacting with the channel walls. At $t = 15$, the constraint imposed by the dashed lines is removed and particles move inside the channel, following the dynamics described by Eq. (4).

III. RESULTS

To characterize the effect of the asymmetry of the channel walls on the overall flux, we fixed $N = 24$, $l = 15$, $d = 3$, and $h = 6$, and performed simulations for different values of the asymmetry coefficient $\alpha \in [-1, 1]$. To reduce statistical noise, instead of directly measuring the outlet flux $\phi(t)$, we introduce an integrated quantity $B(t)$, which we call balance. $B(t)$ is defined as the difference between the cumulative number of particles crossing the rightmost boundary from the left to the right and the ones crossing it in the opposite direction, up to time t . In the continuum limit,

$$\phi(t) = \frac{1}{h} \dot{B}(t) . \quad (5)$$

Asymptotically, we expect that the balance scales linearly in time, and so we estimated the flux from a linear regression fit of the curve $B(t)$ in the linear regime.

Figure 2(a) shows the balance as a function of time for different values of α . Clearly, spontaneous flow emerges

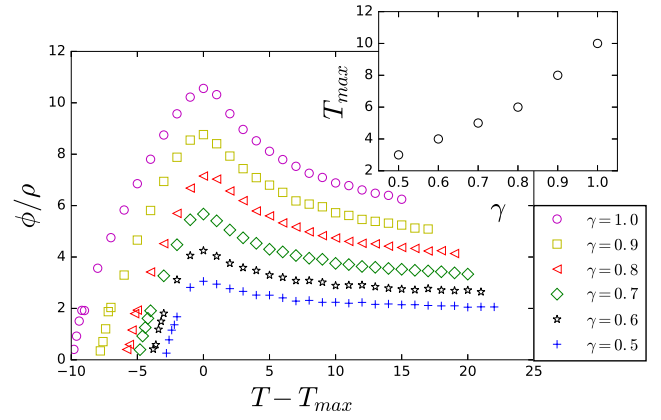


FIG. 5. (Color online) Scaled flux, ϕ/ρ , as a function of the thermostat temperature, for $\alpha = 1$, $\rho = 0.0917$, and different values of the friction constant, γ . The thermostat temperature was shifted by T_{\max} , defined as the optimal temperature at which a maximum is observed in the flux. The dependence of T_{\max} on γ is shown in the inset.

as a result of the asymmetry of the channel walls. For right symmetric channels ($\alpha > 0$), the flow is from the left to the right, while for left symmetric channels ($\alpha < 0$), the flow is in the opposite direction. To analyze the transition at $\alpha = 0$, we define Π as the fraction of samples where $B(t) > 0$ for large values of t ($t = 165$). The dependence of Π on α is in Fig. 2(b), for three different sizes of the channel. One sees that Π is 0.5 for $\alpha = 0$ and it seems to converge to a step function as the system size increases.

The dependence of the flux on the density is shown in Fig. 3(a), for $\alpha = 1$ and $T = 2.5$. One clearly observes an optimal density ($\rho_{\text{opt}} \approx 0.45$) at which the flux is maximized. The data for $\rho < \rho_{\text{opt}}$ suggests two different regimes (see inset of Fig. 3(a)): a low-density regime, for $\rho < 0.1$, and an intermediate-density regime, for $0.1 < \rho < \rho_{\text{opt}}$. Assuming a power-law scaling $\phi \sim \rho^\beta$, we estimate $\beta = 1.47 \pm 0.07$, for the low-density regime, and $\beta = 1.01 \pm 0.04$, for the second one. Figure 3(b) shows the average horizontal component of the velocity (v_x) as a function of the density. For the first regime, v_x increases with the density thus, the enhancement of the flux with the density stems from an increase in the number particles per cell and possible collective effects affecting the particle velocity. By contrast, for the intermediate-density regime, v_x does not significantly change with the density and so the flux only increases due to an increase in the number of particles per cell, yielding a linear scaling. For $\rho > \rho_{\text{opt}}$, a third regime is observed, for which the flux simply decreases with the density due to crowding effects.

To study the dependence on α , we plot in Fig. 4, the flux rescaled by ρ^β , using the estimated values of β for the corresponding regime. We observe a data collapse for each regime, suggesting that the power-law scaling is resilient over the entire range of α values. The low

density regime shows an optimal value of α whereas the intermediate regime shows instead a nearly constant behavior. We think that, for high-enough density, the rate of particle-particle collisions is significantly higher than the one of particle-wall collisions and thus the geometry of the walls does not play a significant role on the overall dynamics. By contrast, for low density, the rates of particle-particle and particle-wall collisions are comparable and a competition between the two is observed, leading to the maximum in the flux.

The dependence of the flux on the thermostat temperature is shown in Fig. 5, for different values of γ . For the entire range of values of γ , a maximum is observed at an optimal temperature, T_{\max} , that increases with γ (see inset). Also, the optimal flux grows with dissipation (increasing γ). Note that, for $\gamma = 0$ the overall flux vanishes and thus a dissipative interaction with the walls is necessary to rectify the thermal motion of gas. This is consistent with the work of Prost *et al.* that suggests that time-reversal symmetry of trajectories needs to be broken to obtain rectification from asymmetric walls [28].

Finally, to quantify the flux for a specific system, let us consider a channel of total length $L = 216 \mu\text{m}$, single cell length $l = 9 \mu\text{m}$, $\alpha = 0$, $p = 1.8 \mu\text{m}$ and $h = 3.7 \mu\text{m}$ at room temperature, with colloidal particles of $\sigma = 6 \times 10^{-7} \text{ m}$, $m = 2.49 \times 10^{-16} \text{ kg}$, and $\gamma = 2 \times 10^{-14} \text{ kg/s}$ [29, 30]. If we assume, $\epsilon/k_b = 0.01414 \text{ K}$ (where k_b is the Boltzmann constant), we obtain a flow velocity $\phi/\rho \approx 42 \mu\text{m/s}$.

IV. CONCLUSION

In this work, we systematically study the dependence of the rectification of the motion of a thermal gas on a

channel of asymmetric dissipative walls. We found that the overall flux enhances with the friction constant of the particle/wall interaction and that it shows a non-monotonic dependence on three other model parameters, namely, the thermostat temperature, channel asymmetry, and particle density. For the dependence of the flux on the density of particles, we found three different regimes. For low density, the flux scales superlinearly with the density, as collective effects lead also to an increase in the horizontal component of particle velocity. For intermediate density, the horizontal component of particle velocity saturates at a constant value and the overall flux scales linearly with the density. Finally, above an optimal value of the density, the flux monotonically decreases due to crowding effects. Future work might consider different geometries and a generalization to the three-dimensional case. The effect of different dissipation mechanisms as well as particle shapes are still open questions.

ACKNOWLEDGMENTS

We acknowledge financial support from the Brazilian institute INCT-SC and grant number FP7-319968 of the European Research Council. NA acknowledges financial support from the Portuguese Foundation for Science and Technology (FCT) under Contract no. UID/FIS/00618/2013 and from the Luso-American Development Foundation (FLAD), FLAD/NSF, Proj. 273/2016.

[1] P. Hänggi and F. Marchesoni, Rev. Mod. Phys. **81**, 387 (2009).
[2] P. Reimann, Phys. Rep. **361**, 57 (2002).
[3] R. Feynman, R. B. Leighton, and M. L. Sands, *The Feynman Lectures on Physics* (Addison-Wesley, 1963) 3 volumes.
[4] H. Leff and A. Rex, *Maxwell's Demon entropy, information and computing* (Princeton University Press, 1990).
[5] P. Hänggi, F. Marchesoni, and F. Nori, Ann.Phys.(Leipzig) **14**, 51 (2005).
[6] I. Derényi and R. D. Astumian, Phys. Rev. E **58**, 7781 (1998).
[7] C. Kettner, P. Reimann, P. Hänggi, and F. Müller, Phys. Rev. E **61**, 312 (2000).
[8] S. Matthias and F. Müller, Nature **424**, 53 (2003).
[9] J. Rousselet, L. Salome, A. Ajdari, and J. Prost, Nature **370**, 446 (1994).
[10] C. Marquet, A. Buguin, L. Talini, and P. Silberzan, Phys. Rev. Lett. **88**, 168301 (2002).
[11] L. P. Faucheux, L. S. Bourdieu, P. D. Kaplan, and A. J. Libchaber, Phys. Rev. Lett. **74**, 1504 (1995).
[12] J. Prost, J.-F. Chauwin, L. Peliti, and A. Ajdari, Phys. Rev. Lett. **72**, 2652 (1994).
[13] G. Costantini, U. Marini Bettolo Marconi, and A. Puglisi, Phys. Rev. E **75**, 061124 (2007).
[14] B. Cleuren and C. V. den Broeck, EPL **77**, 50003 (2007).
[15] C. Van den Broeck, R. Kawai, and P. Meurs, Phys. Rev. Lett. **93**, 090601 (2004).
[16] P. Eshuis, K. van der Weele, D. Lohse, and D. van der Meer, Phys. Rev. Lett. **104**, 248001 (2010).
[17] A. Gnoli, A. Petri, F. Dalton, G. Pontuale, G. Gradenigo, A. Sarracino, and A. Puglisi, Phys. Rev. Lett. **110**, 120601 (2013).
[18] R. Balzan, F. Dalton, V. Loreto, A. Petri, and G. Pontuale, Phys. Rev. E **83**, 031310 (2011).
[19] S. Mobarakabadi, E. N. Oskooee, M. Schröter, and M. Habibi, Phys. Rev. E **88**, 042201 (2013).
[20] L. Angelani, R. Di Leonardo, and G. Ruocco, Phys. Rev. Lett. **102**, 048104 (2009).
[21] R. Di Leonardo, L. Angelani, D. Dell'Arciprete, G. Ruocco, V. Iebba, S. Schippa, M. P. Conte, F. Mecarini, F. De Angelis, and E. Di Fabrizio, Pro-

ceedings of the National Academy of Sciences **107**, 9541 (2010).

[22] A. Sokolov, M. M. Apodaca, B. A. Grzybowski, and I. S. Aranson, Proceedings of the National Academy of Sciences **107**, 969 (2010).

[23] H. Li and H. P. Zhang, EPL **102**, 50007 (2013).

[24] C. L. N. Oliveira, A. P. Vieira, D. Helbing, J. S. Andrade, and H. J. Herrmann, Phys. Rev. X **6**, 011003 (2016).

[25] M.P.Allen and D.J.Tildesley, *Computer simulation of liquids* (Clarendon press, 1989).

[26] T.Poschel and T. Schwager, *Computational Granular Dynamics* (Springer Berlin Heidelberg, 2005).

[27] W. G. Hoover, Phys. Rev. A **31**, 1695 (1985).

[28] J. Prost, J. F. Chauwin, L. Peliti, and A. Ajdari, Phys. Rev. Lett. **72**, 2652 (1994).

[29] A. Tomilov, A. Videcoq, M. Cerbelaud, M. A. Piechowiak, T. Chartier, T. Ala-Nissila, D. Bochicchio, and R. Ferrando, The Journal of Physical Chemistry B **117**, 14509 (2013).

[30] A. Tomilov, A. Videcoq, T. Chartier, T. Ala-Nissila, and I. Vattulainen, The Journal of Chemical Physics **137**, 014503 (2012).